Comparison of ENDF/B-VIII.0 and ENDF/B-VII.1 McCARD Results for Criticality Benchmark and TMI-1 Pin Problems

Ho Jin Park [a*] , Haelee Hyun [a], and Jin Young Cho [a]
[a]*Korea Atomic Energy Research Institute , 111, Daedeok-daero 989beon-gil, Daejeon, 34057, Korea*
[*]*Corresponding author: parkhj@kaeri.re.kr*

1. Introduction

In the reactor physics field, a common Monte Carlo (MC) code uses a continuous energy (CE) cross section library in the ACE format, which is generated from the raw evaluated nuclear data such as ENDF/B, JENDL, and JEFF. This raw evaluated nuclear data library includes cross section data as well as various information for each nuclide (e.g. covariance data, depletion library data). Recently, the Cross Section Evaluation Working Group (CSEWG) released a new revision of ENDF/B evaluated nuclear data library, ENDF/B-VIII.0 [1] and its new format [2].

The purpose of this study is to examine the effects of the newly published ENDF/B-VIII.0 cross sections and their uncertainties on CE criticality calculations in comparison with ENDF/B-VII.1 by McCARD [3] MC calculations. These MC analyses have been performed extensively by analyzing numerous standard criticality benchmark problems for each evaluated nuclear data library.

2. Methods and Results

2.1 ENDF/B-VIII.0 Continuous Energy Cross Section Library Generation

To generate the ENDF/B-VIII.0 CE cross section library in the ACE format, the most up to date NJOY code [4] (i.e. NJOY2016.26) and its user input files for hundreds of nuclides with various temperatures should be prepared. One can access to the newest NJOY source files on its *git* version control software server. We use the ANJOYMC utility program [5] to reduce the user's effort and the possibility of input errors. It provides the easy-to-use functionality for NJOY input decks and a batch file generation. In this study, the neutron CE cross sections are processed by the general flow of data with RECONR, BROADR, UNRESR, PURR, and ACER modules of NJOY code. For each nuclide, the probability tables (PTs) are generated to improve the accuracy of the cross sections in the unresolved resonance energy region. In the same manner, the $S(\alpha,\beta)$ thermal scattering cross sections are generated using RECONR, BROADR, LEAPR, THERMR, and ACER modules. Note that the LEAPR input decks which are provided by the CSEWG are used for $S(\alpha,\beta)$ generation. The library generation procedure is shown in Figure 1. Meanwhile, the neutron sub-library of ENDF/B-VIII.0 has increased to 557 evaluations. In this study, the neutron CE cross section for 550 nuclides are generated by considering three temperature points (300K, 600K and 900K).

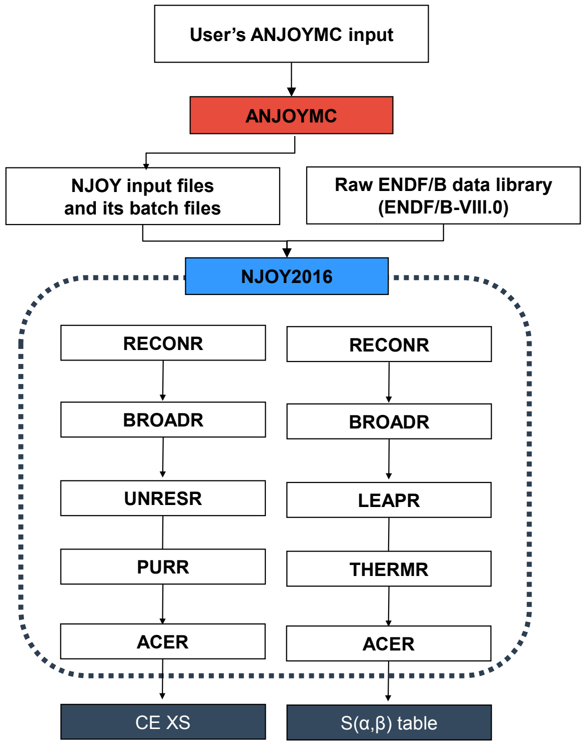

Fig. 1. Flow chart of ENDF/B-VIII.0 CE library generation

2.2 Criticality Benchmark Problem by McCARD

McCARD analyses of the selected International Criticality Safety Benchmark Problems (ICSBEP) [6] are performed with ENDF/B-VIII.0 and ENDF/B-VII.1 to compare them. The selected critical benchmark problems are divided into the four categories due to a type of fuel: plutonium (PU), high enriched uranium (HEU), low enriched uranium (LEU), and ^{233}U (U233). All McCARD calculations are performed by employing 100,000 neutron histories per cycle, 1000 active cycles, and 50 inactive cycles. The statistical uncertainties of k_{eff} values are less than 10 pcm. Table I compares the k_{eff}'s calculated by McCARD with the two evaluated nuclear data libraries. In order to verify the results, the MCNP criticality test results are given in Table I, additionally. In most of the benchmark cases, there are no significant differences between ENDF/B-VIII.0 and ENDF/B-VII.1 results by McCARD except PU cases – PU.

Table I. Comparison of k_{eff}'s calculated by McCARD for each evaluated nuclear data library

Handbook ID	Benchmark	McCARD		MCNP[1]
		ENDF/B-VII.1	ENDF/B-VIII.0	ENDF/B-VIII.0
PU-MET-FAST-001	1.00000 ± 0.00200	0.99981	0.99982	0.99985
PU-MET-FAST-002	1.00000 ± 0.00300	1.00015	1.00136	1.00132
PU-MET-FAST-020	0.99930 ± 0.00170	0.99807	0.99655	0.99637
PU-SOL-THERM-011, case 18-1	1.00000 ± 0.00520	0.99358	0.98785	0.98770
PU-SOL-THERM-011, case 16-5	1.00000 ± 0.00520	1.00614	1.00020	1.00007
PU-SOL-THERM-011, case 16-1	1.00000 ± 0.00520	1.01144	1.00565	1.00349
HEU-MET-FAST-001	1.00000 ± 0.00100	0.99974	1.00020	0.99994
HEU-MET-FAST-028	1.00000 ± 0.00300	1.00278	1.00070	1.00069
HEU-SOL-THERM-013, case 1	1.00120 ± 0.00260	0.99817	0.99842	0.99823
HEU-SOL-THERM-013, case 2	1.00070 ± 0.00360	0.99747	0.99783	-
HEU-SOL-THERM-032	1.00150 ± 0.00260	0.99933	0.99876	0.99842
LEU-COMP-THERM-002, case 1	0.99970 ± 0.00200	0.99909	0.99861	0.99843
LEU-COMP-THERM-002, case 2	0.99970 ± 0.00200	1.00046	0.99988	0.99985
LEU-COMP-THERM-002, case 3	0.99970 ± 0.00200	1.00004	0.99948	0.99946
LEU-COMP-THERM-077	1.00030 ± 0.00100	1.00293	1.00295	-
U233-MET-FAST-001	1.00000 ± 0.00100	0.99993	1.00041	1.00044
U233-MET-FAST-002	1.00000 ± 0.00100	0.99970	1.00099	1.00016
U233-MET-FAST-003	1.00000 ± 0.00100	0.99914	0.99968	0.99967
U233-MET-FAST-006	1.00000 ± 0.00100	0.99873	1.00012	0.99950
U233-SOL-THERM-008	1.00060 ± 0.00290	1.00121	0.99992	0.99974

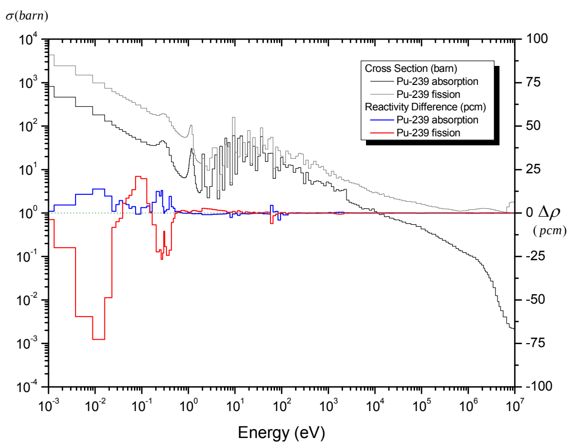

Fig. 2. Comparison of the ^{239}Pu absorption and fission cross section for PU-SOL-THERM011, case 16-5.

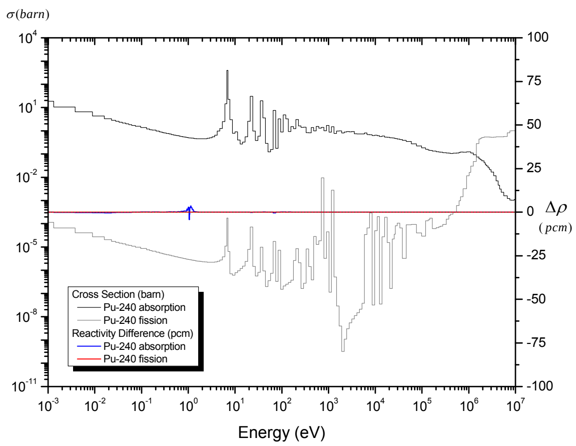

Fig. 3. Comparison of the ^{240}Pu absorption and fission cross section for PI-SOL-THERM011, case 16-5.

To give an understanding on the difference of k_{eff}, the quantitative analysis for the reactivity difference between them in PU-SOL-THERM-011, case 16-5 is preformed and their results are shown in Figs. 2 and 3. In the quantitative analysis, the difference in absorption and fission cross section between ENDF/B-VIII.0 and ENDF/B-VII.1 McCARD results are converted into the reactivity difference in 'pcm' unit for 190 energy group. It is observed that almost all of the difference in the reactivity occur in thermal energy region of ^{239}Pu.

2.3 Uncertainty Quantification in Multiplication Factors for Godiva and TMI-1 Pin Problem

In the McCARD code, the SNU sensitivity and uncertainty (S/U) formulation [7,8] is used to quantify the uncertainty of multiplication factor k. It can cover the statistical uncertainty and the uncertainty caused by MC input data uncertainties. The uncertainty of multiplication factor k due to uncertainties of nuclear cross section input data can be quantified by

$$\sigma_{\mathrm{xx}}^2(k) \cong \sum_{i,\alpha,g}\sum_{i',\alpha',g'} \mathrm{cov}[x_{\alpha,g}^i, x_{\alpha',g'}^{i'}]\left(\frac{\partial k}{\partial x_{\alpha,g}^i}\right)\left(\frac{\partial k}{\partial x_{\alpha',g'}^{i'}}\right) \quad (1).$$

where $x_{\alpha,g}^i$ is the α-type cross section of nuclide i for energy group g and $\mathrm{cov}[x_{\alpha,g}^i, x_{\alpha',g'}^{i'}]$ is the covariance matrix between them. The ERRORR module of NJOY code is used to produce the 30 group covariance matrices from the evaluated nuclear data library. Sensitivity coefficients such as $\partial k/\partial x_{\alpha,g}^i$ can be efficiently calculated by the adjoint flux weighted perturbation (AWP) method [9], which is implemented into the McCARD code. Both ENDF/B-VII.1 and ENDF/B-VIII.0 evaluated nuclear data library contains covariance data (MF31 and 33) for most isotopes. The difference between two covariance data is discussed by identifying the cross section types contributing significantly to the uncertainties of criticality estimates of HEU-MET-FAST-001 (Godiva) and the TMI-1 PWR fuel pin problem [10,11]. Table II displays the contribution of ^{235}U and ^{238}U nuclear data uncertainties of multiplication factor by reaction types. In Godiva, the most significant contributor of ENDF/B-VIII.0 to $\sigma^2_{xx}(k_{eff})$ is the uncertainties of ^{235}U fission cross section (MT=18), whereas that of ENDF/B-VII.1 is the uncertainties of ^{235}U capture cross section (MT=102). Contrastively, in either case, the uncertainty in k_∞ for the TMI-1 pin problem is most affected by the uncertainties of the number of neutrons (ν) per ^{235}U fission (MT=452). The change of the uncertainties in k comes from the difference of the evaluation by each covariance provider. Figure 4 presents the group-wise covariance data of ^{235}U for each evaluated nuclear data library. It is noted that the uncertainties of capture cross section for ENDF/B-VIII.0 is smaller than those for ENDF/B-VII.1 in the whole energy region. This leads to the decrease in the uncertainties of multiplication factor for each problem. On the other hand, the uncertainties of the ^{235}U fission cross section in fast energy region for ENDF/B-VIII.0 is larger than those for ENDF/B-VII.1. For Godiva, the dramatic increase of uncertainty in k_{eff} according to fission cross section can be interpreted as the change of the covariance data. Meanwhile the uncertainties of ν for ENDF/B-VIII.0 is smaller than those for ENDF/B-VII.1 in the fast (0.6 MeV~) and thermal (~100eV) energy region. Consequently, the uncertainty in multiplication factor due to ν of ^{235}U by ENDF/B-VIII.0 is relatively small compared with that by ENDF/B-VII.1 for both Godiva and the TMI-1 pin problem.

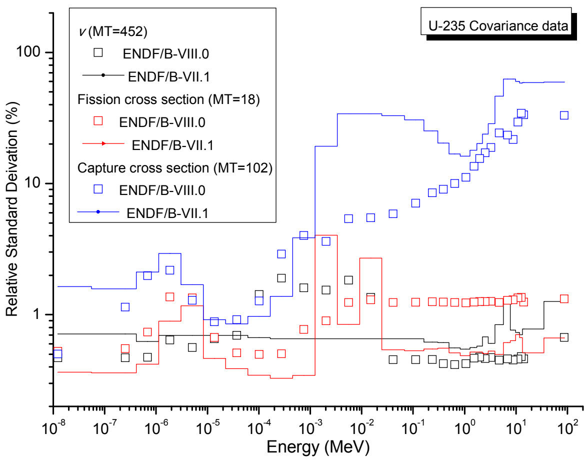

Fig. 4. Comparison of the ^{235}U cross section uncertainties between ENDF/B-VIII.0 and ENDF/B-VII.1

3. Conclusions

In this study, the McCARD criticality and S/U analyses are performed for various criticality benchmarks and the TMI-1 pin problem with the newly published ENDF/B-VIII.0 and the previous version of ENDF/B: ENDF/B-VII.1 library. Overall, it is observed that the prediction performance of criticality is retained except for the plutonium-based thermal system. On the contrary, there have been considerable changes in the covariance data. The changes have a strong correlation with the decreases in the total uncertainty of multiplication factor for Godiva and the TMI-1 pin problem. In the near future, the newly generated ENDF/B-VIII.0 CE cross section library will be tested using more diverse benchmark problems to confirm its improvement.

Table II. Uncertainties of multiplication factors due to the nuclear cross section data uncertainties, $\sigma_{xx}(k)$ (%)

Nuclide	Cov. Data	Godiva		TMI-1 Pin Problem	
		ENDF/B-VII.1	ENDF/B-VIII.0	ENDF/B-VII.1	ENDF/B-VIII.0
^{235}U	ν, ν	0.544	0.399	0.852	0.602
	(n,γ), (n,γ)	0.850	0.280	0.295	0.099
	(n,fis), (n,fis)	0.268	0.784	0.112	0.145
	(n,n), (n,n)	0.294	0.308	0.003	0.002
	(n,n), (n,n')	0.395	0.133	0.001	0.000
	(n,n'), (n,n')	0.660	0.236	0.006	0.001
^{238}U	ν, ν	0.011	0.011	0.103	0.103
	(n,γ), (n,γ)	0.001	0.002	0.417	0.229
	(n,fis), (n,fis)	0.003	0.008	0.022	0.050
	(n,n), (n,n)	0.026	0.017	0.048	0.046
	(n,n), (n,n')	0.053	0.018	0.077	0.014
	(n,n'), (n,n')	0.119	0.027	0.128	0.022
Total		1.194	1.033	0.720	0.482

REFERENCES

[1] D.A. Brown et al, ENDF/B-VIII.0: The 8th Major Release of the Nuclear Reaction Data Library with CIELO-project Cross Sections, New Standards and Thermal Scattering Data, Nuclear Data Sheets, Vol 148, p 1-142, 2018.

[2] "ENDF-6 Formats Manual: Data Formats and Procedures for the Evaluated Nuclear Data Files ENDF/B-VI, ENDF/B-VII and ENDF/B-VIII," Cross Sections Evaluation Working Group, 2018.

[3] H. J. Shim et al., McCARD: Monte Carlo Code for Advanced Reactor Design and Analysis, Nuclear Engineering and Technology, Vol. 44, p 161-176, 2012.

[4] R.E. McFarlance et al., "The NJOY Nuclear Data Prcessing System Version 2016," LA-UR-17-20093, 2016.

[5] K. S. Kim and C. C. Lee, "Devleopment of ANJOYMC Program for Automatic Generation of Monte Carlo Cross Section Libraries," KAERI/TR-3371/2007, 2007.

[6] "International Handbook of Evaluated Criticality Safety Benchmark Experiments," OECD Nuclear Energy Agency report NEA/NSC/COD(95)03, 1998 Edition.

[7] H. J. Park et al., Uncertainty Propagation in Monte Carlo Depletion Analysis, Nuclear Science and Engineering, Vo.167, p. 196-208 , 2011.

[8] H. J. Park et al., Effect of Cross Section Uncertainties on Criticality Benchmark Problem by McCARD, Journal of the Korean Physical Society, Vol. 59, p 1252, 2011.

[9] H. J. Shim and C. H. Kim, Adjoint Sensitivity and Uncertainty Analyses in Monte Carlo Forward Calculations, J. Nucl. Sci. Technol., Vol.48, p.1453-1461, 2011.

[10] K. Ivanov et al., "Benchmark for Uncertainty Analysis in Modeling (UAM) for Design, Operation and Safety Analysis of LWRs, Volume I: Specification and Support Data for the Neutronics Cases (Phase I)," NEA/NSC/DOC(2012), OECD Nuclear Energy Agency, 2012.

[11] H. J. Park, H. J. Shim, and C. H. Kim, Uncertainty Propagation Analysis for PWR Burnup Pin-Cell Benchmark by Monte Carlo Code McCARD, Science and Technology of Nuclear Installations, Vol 2012, Article ID 616253, 2012.